

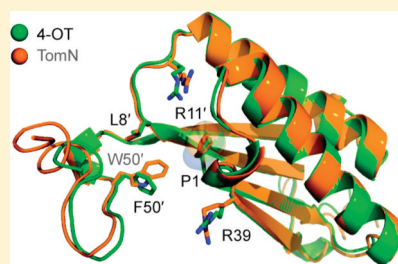
Kinetic, Crystallographic, and Mechanistic Characterization of TomN: Elucidation of a Function for a 4-Oxalocrotonate Tautomerase Homologue in the Tomaymycin Biosynthetic Pathway

Elizabeth A. Burks,[†] Wupeng Yan,[‡] William H. Johnson, Jr.,[†] Wenzong Li,[‡] Gottfried K. Schroeder,[†] Christopher Min,[§] Barbara Gerratana,[§] Yan Zhang,^{*,‡} and Christian P. Whitman^{*,†}

[†]Division of Medicinal Chemistry, College of Pharmacy, and [‡]Department of Chemistry and Biochemistry, University of Texas, Austin, Texas 78712, United States

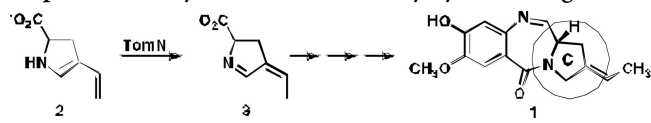
[§]Department of Chemistry and Biochemistry, University of Maryland, College Park, Maryland 20742, United States

ABSTRACT: The biosynthesis of the C ring of the antitumor antibiotic agent, tomaymycin, is proposed to proceed through five enzyme-catalyzed steps from L-tyrosine. The genes encoding these enzymes have recently been cloned and their functions tentatively assigned, but there is limited biochemical evidence supporting the assignments of the last three steps. One enzyme, TomN, shows 58% pairwise sequence similarity with 4-oxalocrotonate tautomerase (4-OT), an enzyme found in a catabolic pathway for aromatic hydrocarbons. The TomN sequence includes three amino acids (Pro-1, Arg-11, and Arg-39) that have been identified as critical catalytic residues in 4-OT. However, the proposed substrate for TomN is very different from that processed by 4-OT. To establish the function and mechanism of TomN and its relationship with 4-OT, we conducted kinetic, mutagenic, and structural studies. The kinetic parameters for TomN, and four alanine mutants, P1A, R11A, R39A, and R61A, were determined using 2-hydroxy-2,4-hexadienedioate, the substrate for 4-OT. The TomN-catalyzed reaction using this substrate compares favorably to that of 4-OT. In addition, the kinetic parameters for the P1A, R11A, and R39A mutants of TomN parallel the trends observed for the corresponding 4-OT mutants, implicating an analogous mechanism. A high-resolution crystal structure (1.4 Å) of TomN shows that the overall structure and the active site region are highly similar to those of 4-OT with a root-mean-square deviation of 0.81 Å. Moreover, key active site residues are positionally conserved. The combined results suggest that the tentative assignment for TomN and the proposed sequence of events in the biosynthetic pathway leading to the formation of the C ring of tomaymycin might not be correct. An alternative pathway that awaits biochemical confirmation is proposed.



Pyrrolo[1,4]benzodiazepine (PBD) natural products such as anthramycin, sibiromycin, and tomaymycin [1 (Scheme 1)]

Scheme 1. Proposed TomN-Catalyzed Reaction, a Putative Step in the Biosynthesis of the Tomaymycin C Ring

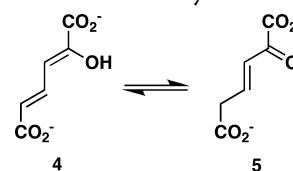


are noted for their antitumor and antibiotic activities, resulting from sequence-specific DNA alkylation.^{1,2} Interest in their anticancer properties has spawned the design, synthesis, and characterization of numerous PBD derivatives and the recent cloning of the biosynthetic gene clusters for sibiromycin and tomaymycin.³ Biochemical characterization of the individual enzymes making up these biosynthetic pathways and manipulation of the corresponding genes can expand the repertoire of PBD analogues to include synthetically inaccessible ones.^{1–3}

One step in the biosynthesis of the tomaymycin C ring is catalyzed by the 4-oxalocrotonate tautomerase (4-OT) homologue designated TomN.¹ It is proposed that TomN converts 4-vinyl-2,3-dihydropyrrole-2-carboxylic acid (2) to

4-ethylidene-3,4-dihydropyrrole-2-carboxylic acid (3). The putative TomN substrate is very different from the one processed in the canonical 4-OT-catalyzed reaction, which involves the conversion of 2-hydroxy-2,4-hexadienedioate or 2-hydroxy-2,4-hexadienedioate [4 (Scheme 2)] to 2-oxo-3-hexenedioate

Scheme 2. Canonical 4-OT-Catalyzed reaction



(5).^{4,5} Moreover, TomN is found in a biosynthetic pathway, whereas 4-OT is part of a catabolic pathway in *Pseudomonas putida* mt-2, *Pseudomonas* sp. CF600, and other soil bacteria.⁶ These two observations led to our interest in the enzymes of the tomaymycin and related biosynthetic pathways.

Received: June 20, 2011

Revised: July 27, 2011

Published: August 2, 2011

Kinetic, mechanistic, and structural studies identified Pro-1, Arg-11, Arg-39, and Phe-50 as key players in the 4-OT-catalyzed conversion of **4** to **5**.^{7–15} In the proposed mechanism, Pro-1, which has a pK_a of ~ 6.4 , transfers a proton from the 2-hydroxy group of **4** to C-5 of **5**.^{7–10} The interaction between Arg-11 and the C-6 carboxylate group is proposed to bind the substrate and draw electron density to C-5 to facilitate protonation at this position.^{11,12,14,15} Arg-39 may interact with the 2-hydroxy group and a carboxylate oxygen of C-1. Mutagenesis results suggest that its role is primarily catalytic, where the positively charged guanidinium moiety might stabilize the developing carbanionic character after deprotonation of the 2-hydroxy group. Phe-50 is a major contributor to a hydrophobic pocket near the prolyl nitrogen of Pro-1.^{13,15} The proximity of the pocket is largely responsible for the unusually low pK_a of Pro-1.

The TomN sequence has 66 amino acids (with Pro-1, Arg-11, and Arg-39 conserved, but Phe-50 replaced with tryptophan) and is $\sim 58\%$ similar ($\sim 33\%$ identical) to that of 4-OT (from *P. putida* mt-2).¹ In view of the high degree of similarity and the presence of the conserved key residues, notably Arg-11 and Arg-39, it is somewhat odd that the proposed substrate for TomN has one carboxylate group, whereas the known substrate for 4-OT has two carboxylate groups. This observation raises two possibilities. The proposed substrate for TomN is not correct, or our understanding of the functions played by the two arginine residues in the canonical 4-OT-catalyzed reaction is not complete.

To address these issues, we characterized TomN using **4** [proposed substrate for TomN (i.e., **2**) not available¹]. It was found that **4** is a substrate for TomN with kinetic parameters that are comparable to those of 4-OT (using **4**). Mutagenesis studies implicate Pro-1, Arg-11, and Arg-39 as critical residues in this TomN-catalyzed reaction, suggesting a mechanism analogous to that of 4-OT. Finally, a crystal structure (1.40 Å resolution) indicates that the fold and active site of TomN are very similar to those of 4-OT, with a root-mean-square deviation (rmsd) of the main chain of 0.81 Å. Our results suggest that the proposed TomN substrate might not be correct, and that the actual substrate might resemble a molecule with the 2-hydroxymuconate framework (i.e., **4**). These observations impact the tentatively assigned functions of the enzymes involved in the biosynthesis of the C ring of tomaymycin.

EXPERIMENTAL PROCEDURES

Materials. Chemicals, biochemicals, buffers, and solvents were purchased from Sigma-Aldrich Chemical Co. (St. Louis, MO), Fisher Scientific Inc. (Pittsburgh, PA), Fluka Chemical Corp. (Milwaukee, WI), or EM Science (Cincinnati, OH). The syntheses of 2-hydroxymuconate (**4**),⁴ 5-(methyl)-2-hydroxymuconate (**6**),¹⁶ 5-(carboxymethyl)-2-hydroxymuconate (**8**),¹⁷ 2-hydroxy-2,4-pentadienoate (**9**),¹⁸ 2-hydroxy-2,4-heptadiene-1,7-dioate (**12**),¹⁹ and 2-oxo-3-pentynoate (**17**)²⁰ have been reported previously. Recombinant 4-OT was purified by previously reported procedures.^{15,21} Sequencing grade endoproteinase Glu-C (protease V-8) from *Staphylococcus aureus* was obtained from Sigma-Aldrich Chemical Co. The Phenyl Sepharose 6 Fast Flow and DEAE-Sepharose resins and the prepacked PD-10 Sephadex G-25 columns were obtained from GE Healthcare (Piscataway, NJ). The Econo-Column chromatography columns and Freeze 'N Squeeze units were obtained from Bio-Rad Laboratories, Inc. (Hercules, CA). Enzymes and

reagents used for molecular biology procedures were obtained from New England Biolabs, Inc. (Ipswich, MA).

Bacterial Strains, Plasmids, and Growth Conditions.

Escherichia coli strain DH5 α was obtained from Invitrogen (Carlsbad, CA). *E. coli* strain BL21-Gold(DE3) was obtained from Stratagene (La Jolla, CA). The pET vectors were obtained from Novagen (Madison, WI). Plasmids were isolated from cell cultures using the Sigma GenElute Plasmid Miniprep Kit or the Qiagen QIAprep Spin Miniprep Kit. Cells for cloning and overproduction were grown on Luria-Bertani (LB) agar plates or in LB medium supplemented with kanamycin (Kn) (30 $\mu\text{g/mL}$). The sources for the components of Luria-Bertani medium have been reported previously.²²

General Methods. Techniques for restriction enzyme digestion, ligation, transformation, and other standard molecular biology manipulations were based on methods described previously.²² Oligonucleotide primers were synthesized by Sigma-Aldrich. DNA sequencing was performed at the DNA core facility of the Institute for Cellular and Molecular Biology (ICMB) at the University of Texas. Mass spectral data were obtained on an LCQ electrospray ion-trap mass spectrometer (Thermo, San Jose, CA) in the ICMB Protein and Metabolite Analysis Facility at the University of Texas. Samples were prepared as described previously.²³ A Voyager-DE Pro matrix-assisted laser desorption ionization (MALDI) mass spectrometer (PerSeptive Biosystems, Framingham, MA) was used to determine peptide masses. Kinetic data were obtained at 24 °C on an Agilent 8453 diode-array spectrophotometer. Nonlinear regression data analysis was performed using Graft (Erithacus Software Ltd., Staines, U.K.) obtained from Sigma-Aldrich. Protein concentrations were determined by the method described by Waddell.²⁴ Protein was analyzed by tricine sodium dodecyl sulfate–polyacrylamide gel electrophoresis (SDS–PAGE) on 15% T/2% C gels on a Bio-Rad Mini-Protein II gel electrophoresis apparatus.²⁵ Nuclear magnetic resonance (NMR) spectra were recorded in 100% H₂O on a Varian Unity INOVA-500 spectrometer as reported previously.^{15,23}

Cloning of the *tomN* Gene into the pET24 Vector. The *tomN* gene was previously cloned into the pRSF Duet 1 vector between the *NdeI* and *EcoRV* restriction sites with a unique *XhoI* site downstream. The pRSF Duet 1 vector containing *tomN* and an aliquot of pET24 were digested with the *NdeI* and *XhoI* restriction enzymes. The two digestion mixtures were electrophoresed on an agarose gel and the appropriate pieces recovered using a Freeze 'N Squeeze unit followed by ethanol precipitation and centrifugation. After ligation with T4 DNA ligase, the product was used to transform *E. coli* DH5 α cells by electroporation using a Bio-Rad MicroPulser Electroporation unit. The transformation reaction mixture was plated on LB/Kn plates and grown overnight at 37 °C. Following PCR screening, two positive colonies were used to start individual overnight cultures from which the plasmid was isolated and sequenced.

Construction of the TomN Mutants. Four TomN mutants (P1A, R11A, R39A, and R61A) were constructed. Two mutants (R11A and R61A) were constructed by a PCR method that is based on the Stratagene QuikChange and New England Biolabs Phusion site-directed mutagenesis systems. Wild-type TomN in the pRSF Duet 1 vector served as the template with the following primer pairs (forward and reverse, respectively), where the mutation site is underlined. For the R11A mutant, primer 1 was 5'-CCTTGCTGGAG-GGCGCGTCGCCGAGGAGGTG-3' and primer 2 was

5'-CACCTCTGCGGCGACGCGCCCTCCAGCAAGG-3'. For the R61A mutant, primer 3 was 5'-GGCCGAGCG-GGCGGCCTCCCCCTCG-3' and primer 4 was 5'-CGAGG-GGGAGGCCGCCGCTCGGCC-3'.

For the R11A mutant, the PCR mixture (50 μ L) contained *tomN* in the pRSF plasmid (50 ng), primers 1 and 2 (125 ng each), 5 \times Phusion GC buffer supplied with the polymerase (10 μ L), dNTPs (0.2 mM each), and NEB Phusion DNA polymerase (1 unit). The reaction mixture was processed in a heated top PCR thermocycler using a protocol that consisted of an initial 30 s denaturation cycle at 95 $^{\circ}$ C, followed by 18 cycles of 95 $^{\circ}$ C for 30 s, 55 $^{\circ}$ C for 1 min, and 72 $^{\circ}$ C for 7 min, and ended with a hold at 4 $^{\circ}$ C. Following the PCR, *DpnI* restriction enzyme (1 μ L of a 20 unit/ μ L solution) was added to the mixture to digest the methylated parent plasmid. After the mixture had been incubated for 2 h at 37 $^{\circ}$ C, the DNA was precipitated, suspended in 10 mM Tris chloride buffer (pH 8.5), and added to *E. coli* DH5 α cells (40 μ L) for electroporation. The transformed cells were selected by overnight growth at 37 $^{\circ}$ C on LB/Kn plates. Two colonies were chosen and grown overnight in LB/Kn medium at 37 $^{\circ}$ C. The plasmid was isolated and sequenced to confirm that only the desired mutation was present. Subsequently, the gene was transferred to pET24 in the same manner as described above for the wild type. The R61A mutant of TomN was constructed similarly except the *DpnI*-digested product was recovered and treated with T4 DNA ligase for 10 min (in ligase buffer). The DNA was recovered and added to the *E. coli* DH5 α cells for electroporation.

The P1A and R39A mutants were constructed by overlap extension PCR, as described below and elsewhere.²⁶ Wild-type TomN was amplified from the pET24 construct using primers 5 and 6 (5'-CATGAGCCCCGAAGTGGCGAGC-3' and 5'-GC-TAGTTATTGCTCAGCGG-3', respectively), where primer 5 (the forward primer) is specific for a region slightly upstream of the T7 promoter sequence and primer 6 (the reverse primer) is complementary to a region immediately upstream of the T7 terminator region of the pET24 plasmid. The PCR mixture (50 μ L) contained wild-type TomN in the pET24 plasmid (62 ng), primers 5 and 6 (0.2 μ M each), 10 \times Thermo buffer supplied with the polymerase (5 μ L), dNTPs (0.2 mM each), and NEB Taq polymerase (1.5 units). The reaction mixture was processed in the heated top PCR thermocycler using a protocol that consisted of an initial 2 min denaturation cycle at 94 $^{\circ}$ C, followed by 29 cycles of 94 $^{\circ}$ C for 1 min, 55 $^{\circ}$ C for 2 min, and 72 $^{\circ}$ C for 3 min, and ended with an elongation step at 72 $^{\circ}$ C for 10 min and a hold at 4 $^{\circ}$ C. The product was treated with *DpnI* restriction enzyme; the reaction mixture was electrophoresed, and the desired band was excised and processed through a Freeze 'N Squeeze unit to recover the TomN coding region. The individual pieces required for overlap extension for the P1A and R39A mutants were generated in separate PCRs. Each PCR mixture (50 μ L) contained the TomN coding region (1 μ L from the Freeze 'N Squeeze unit), the pair of primers indicated below (0.2 μ M each), 10 \times Thermo buffer (5 μ L), dNTPs (0.2 mM each), and NEB Taq polymerase (1.5 units). Each reaction was conducted using the PCR conditions described above. For the P1A mutant, primer 7 was 5'-GATATACATA-TGGCGCTCATCCGCGTCAC-3', primer 8 was 5'-GTGAC-GCGGATGAGCGCCATATGTATATC-3', and primer 9 was 5'-S'GATCCCGCGAAATTAATACGAC-3'. For the R39A mutant, primer 10 was 5'-GGCCGTCGCGGTGATCGTGGAGGAG-3', primer 11 was 5'-CTCCTCCACGATCACCGCGACGGCC-3',

and primer 6 is described above. The 5'-piece for the P1A mutant was constructed using primers 8 and 9. The 3'-piece was constructed using primers 6 and 7. The 5'-piece for the R39A mutant was constructed using primers 9 and 11. The 3'-piece was constructed using primers 6 and 10. Primer 9 is specific for part of the T7 promoter sequence and immediately upstream of that sequence in pET24. Each reaction mixture was electrophoresed, and the desired band was excised and processed through a Freeze 'N Squeeze unit and used in subsequent PCR mixtures, as follows. The PCR mixture (50 μ L) for overlap extension contained the 5'-piece that eluted from the Freeze 'N Squeeze unit (1 μ L), the 3'-piece that eluted from the Freeze 'N Squeeze unit (3 μ L for the P1A mutant and 1 μ L for the R39A mutant), primers 6 and 9 (0.2 μ M each), 10 \times Thermo buffer (5 μ L), dNTPs (0.2 mM each), and NEB Taq polymerase (1.5 units). The reaction mixture was processed in the heated top PCR thermocycler and the overlap product recovered as described above. To generate sufficient material for insertion into the pET24 vector, each overlap product was further amplified in four 50 μ L PCRs using the overlap product (1 μ L) as the template. The reaction products were pooled and the products recovered as described above, followed by ethanol precipitation and centrifugation. Each product (containing the mutation) was cloned into the pET24 vector between the *NdeI* and *XhoI* restriction sites following the procedures described for the cloning of the wild-type gene into the pET24 vector. For each mutant, one colony was grown for the plasmid, which was sequenced and subsequently used to transform *E. coli* BL21-Gold(DE3) cells for protein expression.

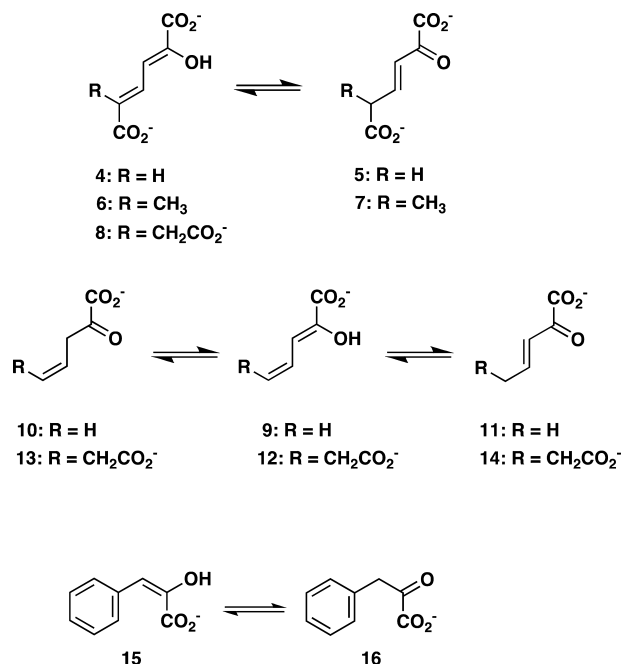
Expression and Purification of TomN and the TomN Mutants. Several colonies (i.e., a streak) of the pET vector construct (encoding TomN or a TomN mutant) transformed in *E. coli* BL21-Gold(DE3) cells were used to inoculate LB/Kn medium (~20 mL). After the cells had been shaken overnight at 37 $^{\circ}$ C, an aliquot was used to inoculate LB/Kn medium (~550 mL) in a 2 L flask so that the initial OD₆₀₀ reading was ~0.05. Cells were allowed to grow at 37 $^{\circ}$ C with shaking until the OD₆₀₀ reached ~1 (~2 h) and then induced by the addition of isopropyl β -D-thiogalactoside (IPTG) (final concentration of 0.5 mM). After growing for an additional 3 h, the cells were collected by centrifugation (15 min at 11000g) at 4 $^{\circ}$ C and stored at -80 $^{\circ}$ C. Typically, ~11.8 g of cells was collected from eight 550 mL cultures.

The purification protocol was adapted from previously described ones and modified as follows.^{15,21} In a typical procedure, cells (~13.4 g) were thawed and suspended in ~40 mL of 20 mM HEPES buffer (pH 7.6) containing 0.1 M KCl (buffer A). The cells were sonicated and centrifuged as described previously,^{15,21} to yield ~38 mL of supernatant. The supernatant was diluted to 120 mL with buffer A, placed on ice, and stirred while (NH₄)₂SO₄ (~31 g) was added slowly to make a 45% saturated solution. After being stirred for 30 min, the sample was centrifuged (10 min at 10000 rpm), and the pellet was discarded. The supernatant was loaded onto a Phenyl-Sepharose column (8 mL of resin) equilibrated with 45% saturated (NH₄)₂SO₄ in 20 mM HEPES buffer (pH 7.6). After the sample had been loaded, the column was washed with equilibrating buffer (40 mL) followed by a linear gradient [160 mL total, 80 mL of 45% saturated (NH₄)₂SO₄ in 20 mM HEPES buffer (pH 7.6) to 80 mL of buffer with no (NH₄)₂SO₄]. Fractions (~0.8 mL) were collected and analyzed for

activity using 2-hydroxymuconate (**4**). Fractions containing the highest activity were pooled and diluted 20-fold with 20 mM HEPES buffer (pH 7.6). The resulting solution was loaded onto a DEAE-Sepharose column (8 mL of resin) that had been equilibrated with 20 mM HEPES buffer (pH 7.6) containing 0.1 M KCl. After the column had been washed with 5 column volumes of equilibrating buffer, a linear gradient [160 mL total, 0.1 to 0.5 M KCl in 20 mM HEPES buffer (pH 7.6)] was used to elute the protein. Active fractions were identified by the activity with **4** and examined for purity using tricine SDS-PAGE. Typically, this procedure yields ~19 mg of TomN purified to >95% homogeneity (as assessed by SDS-PAGE). The enzyme or mutant enzyme was exchanged into assay buffer using a PD-10 column, per the manufacturer's instructions.

Enzyme Assays and Kinetic Studies Using TomN and TomN Mutants. The activities of wild-type TomN were examined using **4**, **6**, **8**, **9**, **12**, and **15** (Scheme 3). TomN

Scheme 3. Known Tautomerase Superfamily Substrates Examined as Substrates for TomN



processed all except for **8**. Accordingly, the kinetic parameters were measured for the substrates processed in 10 mM potassium phosphate buffer (pH 7.3), as follows, and are reported in Table 1. The ketonization of **4** to **5** (by TomN) was measured by following the increase in absorbance at 236 nm ($\epsilon = 6580 \text{ M}^{-1} \text{ cm}^{-1}$) using substrate concentrations ranging from 20 to 200 μM with an enzyme concentration of 4 nM.⁴ The ketonization of **6** to **7** (by TomN and 4-OT) was measured by following the increase in absorbance at 236 nm ($\epsilon = 18500 \text{ M}^{-1} \text{ cm}^{-1}$) using substrate concentrations ranging from 40 to 400 μM with enzyme concentrations of 317 nM (TomN) and 18 nM (4-OT).⁴ For **6**, the composition of an equilibrium mixture (43% **6**, 24% **7**, and 33% 5-methyl-2-oxo-4-hexenedioate) was determined by ¹H NMR spectroscopy. The ketonization of **9** to **10** was measured by following the decrease in absorbance at 265 nm ($\epsilon = 12700 \text{ M}^{-1} \text{ cm}^{-1}$) using substrate concentrations ranging from 20 to 160 μM with an enzyme concentration of 3000 nM (TomN) or 18 nM (4-OT).

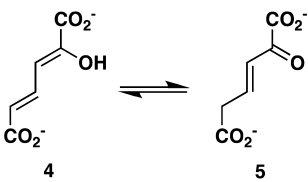
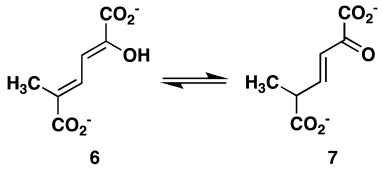
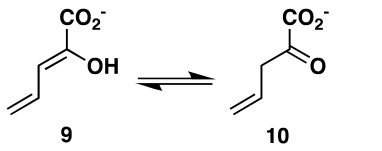
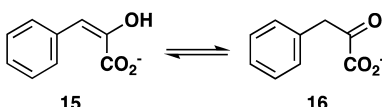
The ketonization of **12** to **13** was measured by following the decrease in absorbance at 276 nm ($\epsilon = 15900 \text{ M}^{-1} \text{ cm}^{-1}$) using substrate concentrations ranging from 20 to 100 μM with an enzyme concentration of 92 nM¹⁹ (data not shown). The ketonization of **15** to **16** was measured by following the decrease in absorbance at 284 nm ($\epsilon = 11500 \text{ M}^{-1} \text{ cm}^{-1}$) using substrate concentrations ranging from 10 to 100 μM with an enzyme concentration of 160 nM.²⁷ Stock solutions (20 mM) of 2-hydroxymuconate (**4**), 5-methyl-2-hydroxymuconate (**6**), 2-hydroxy-2,4-pentadienoate (**9**), 2-hydroxy-2,4-heptadiene-1,7-dioate (**12**), and phenylenolpyruvate (**15**) were made in ethanol. Reactions were initiated by the addition of substrate. The TomN mutants were assayed following the ketonization of **4** to **5** (at 236 nm) using substrate concentrations ranging from 20 to 200 μM with enzyme concentrations of 2.2 μM (P1A), 0.73 μM (R11A), 7.6 μM (R39A), and 40 nM (R61A), and the results are reported in Table 2.

The ketonization of **9** to **11** and that of **12** to **14** in the presence of TomN were examined under conditions that gave complete conversion of substrate to product (i.e., **9** to **11** and **12** to **14**) using 4-OT. Accordingly, the enzyme (~40 μg) was added to a cuvette containing 10 mM potassium phosphate buffer (pH 7.3). The reaction was initiated by the addition of a 7 μL aliquot of **9** or **12** from a 20 mM stock solution and followed for 10 min (**9**) or 2 min (**12**).

Inactivation of TomN by 2-Oxo-3-pentynoate (17**).** 2-Oxo-3-pentynoate [**17**, 1.9 mg (Scheme 4)] was dissolved in 0.3 mL of 100 mM Na₂HPO₄ buffer (pH ~9.5) and then diluted by the addition of water (0.7 mL). After the addition of **17**, the pH of the reaction mixture decreased to ~7. A 50 μL aliquot of this stock solution was added to a 10 mL solution of TomN (~1 mg/mL), the solution inverted, and the resulting mixture incubated at 4 °C for ~15 min. An aliquot (2 μL) was removed and assayed for activity using **4**. Subsequently, an additional 25 μL aliquot of the inhibitor stock solution was added to the enzyme solution, the solution inverted, and the resulting mixture incubated at 4 °C for 15 min. An aliquot (2 μL) was removed and assayed for activity using **4**. A final 15 μL aliquot of the inhibitor stock solution was added, and the mixture was treated as described above. The activity assay showed that TomN was inactivated by a total of 90 μL of the inhibitor solution. The inactivated enzyme was concentrated to 1 mL in an Amicon stirred cell concentrator [1000 molecular weight (MW) cutoff]. The resulting solution was desalted with a PD-10 Sephadex G-25 gel filtration column prewashed with ~50 mL of 10 mM NH₄HCO₃ buffer (pH ~8). Fractions (0.3 mL) were tested for protein content using the Bradford reagent.²⁸ Fractions containing the highest protein concentrations were combined and an aliquot directly infused in the ESI mass spectrometer.

Peptide Mapping and MALDI Mass Spectrometry (MALDI-MS) Analysis. A quantity of TomN [200 μL of a 5.5 mg/mL solution in 10 mM KH₂PO₄ buffer (pH 7.3)] was incubated with **17** [50 μL of a 7 mg/mL solution in 100 mM Na₂HPO₄ buffer (pH ~7)] for 30 min. An aliquot (50 μL) of a NaBH₄ solution [100 mg in 100 mM Na₂HPO₄ buffer (pH ~10)] was added. After 1 h, the solution was concentrated and exchanged into 100 mM NaH₂PO₄ buffer (pH 7.0) (a total of three times), using an Amicon Ultra (3000 MW cutoff) centrifugal filter unit. The residual liquid was diluted to 200 μL with 100 mM NaH₂PO₄ buffer (pH 7.0), and a second aliquot (50 μL) of the solution of **17** was added. After 30 min, 50 μL of

Table 1. Kinetic Parameters for TomN, 4-OT, and hh4-OT Using Dienol and Enol Substrates^a

Reaction	Enzyme	k_{cat} (s ⁻¹)	K_{m} (μM)	$k_{\text{cat}}/K_{\text{m}}$ (M ⁻¹ s ⁻¹)
	TomN ^b	1850 ± 630	512 ± 225	3.6 × 10 ⁶
	4-OT ^c	4000 ± 182	62 ± 8	6.5 × 10 ⁷
	hh4-OT ^c	3000 ± 100	70 ± 8	4.3 × 10 ⁷
	TomN	8.8 ± 0.7	306 ± 45	2.9 × 10 ⁴
	4-OT	111 ± 6	125 ± 17	8.9 × 10 ⁵
	TomN	0.9 ± 0.13	231 ± 41	3.9 × 10 ³
	4-OT	176 ± 20	160 ± 26	1.1 × 10 ⁶
	TomN	16 ± 3.0	334 ± 90	4.8 × 10 ⁴
	4-OT	73 ± 6	199 ± 23	3.7 × 10 ⁵
	hh4-OT ^c	13 ± 1	121 ± 20	1.1 × 10 ⁵

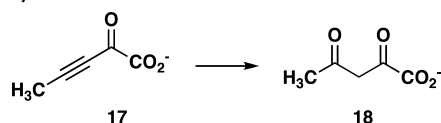
^aThe steady-state kinetic parameters were determined under the conditions described in the text. ^bErrors are standard deviations. ^cThe kinetic parameters are from ref 15.

 Table 2. Kinetic Parameters for TomN, 4-OT, and Mutants Using 4^a

enzyme	k_{cat} (s ⁻¹)	K_{m} (μM)	$k_{\text{cat}}/K_{\text{m}}$ (M ⁻¹ s ⁻¹)
TomN ^b	1850 ± 630	512 ± 225	3.6 × 10 ⁶
4-OT	4000 ± 182	62 ± 8	6.5 × 10 ⁷
P1A-TomN	1.5 ± 0.1	180 ± 10	8.3 × 10 ³
P1A-4-OT ^c	60 ± 3	100 ± 12	6.0 × 10 ⁵
R11A-TomN	14 ± 3	1050 ± 240	1.3 × 10 ⁴
R11A-4-OT ^d	40 ± 6	1600 ± 300	2.5 × 10 ⁴
R39A-TomN	0.20 ± 0.02	440 ± 60	4.5 × 10 ²
R39A-4-OT ^d	28 ± 2	290 ± 40	9.7 × 10 ⁴
R61A-TomN	360 ± 5.0	780 ± 155	4.6 × 10 ⁵
R61A-4-OT ^d	3500 ± 240	290 ± 40	1.2 × 10 ⁷

^aThe steady-state kinetic parameters for TomN and TomN mutants were determined under the conditions described in the text. ^bErrors are standard deviations. ^cThe kinetic parameters are from ref 8. ^dThe kinetic parameters are from ref 11.

Scheme 4. Conversion of 2-Oxo-3-pentynoate to Acetopyruvate, a Diagnostic Reaction for Tautomerase Superfamily Members with a Cationic Pro-1



the NaBH₄ solution was added. After 1 h, the mixture was desalted as described above and analyzed by electrospray ion-trap spectrometry (ESI-MS) to verify covalent modification of the protein. Subsequently, samples of unmodified or modified TomN (50 μL each) were concentrated to dryness using a Speed Vac concentrator, and the residue was dissolved in 3 μL of a saturated guanidine hydrochloride solution. After a 1 h incubation period at 37 °C, the individual mixtures were diluted to 30 μL with 10 mM NaH₂PO₄ buffer (pH 4.0) and treated with 20 μL of a protease V-8 solution [50 μg dissolved in 50 μL of 10 mM NaH₂PO₄ buffer (pH 4.0)]. After a 48 h incubation period at 37 °C, the resulting peptide mixtures were analyzed by MALDI-MS, as previously described.¹⁴

Crystallization and Determination of the Structure of TomN. TomN was purified as described above and then concentrated to ~10 mg/mL in 20 mM HEPES buffer (pH 7.6) containing 300 mM KCl. Several crystallization conditions were identified by the sitting drop method of vapor diffusion. The two conditions resulting in the best diffraction-quality crystals used in this specific study were 100 mM magnesium acetate with 100 mM sodium acetate in 5–21% PEG 8000 (pH 4.5) and 100 mM calcium acetate with 100 mM sodium acetate in 1–13% PEG 4000 (pH 4.5). A crystal from the crystallization drop was transferred to mother liquor with 30% (v/v) glycerol as the cryoprotectant before being frozen in liquid nitrogen for data collection. The X-ray diffraction data were collected at a wavelength of 1 Å at ~100 K on beamline

8.3.1 of the Advanced Light Source (ALS, Berkeley, CA). The data were processed and scaled using HKL2000.²⁹ The data collection statistics are listed in Table 3.

Table 3. Data Collection and Refinement Statistics for TomN

Data Collection	
space group	I4 ₁ 32
cell dimensions	
<i>a</i> , <i>b</i> , <i>c</i> (Å)	117.637, 117.637, 117.637
α , β , γ (deg)	90, 90, 90
resolution (Å)	83.2–1.4 (1.42–1.40)
<i>R</i> _{sym} (%)	7.5 (22.5) ^a
<i>I</i> / σ <i>I</i>	76.9 (1.8) ^a
completeness (%)	100 (100) ^a
Refinement	
resolution (Å)	83.2–1.4
no. of reflections	26052
<i>R</i> _{work} / <i>R</i> _{free} (%)	22.4/25.6
no. of atoms	
protein	964
water	172
<i>B</i> factor (Å ²)	
protein	18.33
water	35.07
rmsd	
bond lengths (Å)	0.028
bond angles (deg)	2.34
Ramachandran plot (%)	
residues in most favored regions	96.2
residues in additional allowed regions	3.8
residues in generously allowed regions	0
residues in disallowed regions	0

^aData for the last resolution shell are given in parentheses.

The TomN structure was determined by molecular replacement (MR) using the 4-OT model (Protein Data Bank entry 1BJP) as the search model. MR solutions were refined with REFMAC in the CCP4 Program Suite.³⁰ The final models were evaluated by PROCHECK.³¹ Refinement statistics are summarized in Table 3. The figures were prepared with PyMol,³² as noted in the figure legends.

RESULTS

Identification of TomN as a Tautomerase Superfamily Member. The TomN sequence was uncovered by a BLAST search of the NCBI database using the sequence of the α -subunit of the heterohexameric 4-OT (hh4-OT) from *Chloroflexus aurantiacus* J-10-fl as the query sequence.¹⁵ (The sequence for the tomaymycin gene cluster is deposited in GenBank and the gene for TomN annotated.¹) The sequence of TomN is 48% identical with that of the α -subunit of hh4-OT (65% similar) and 33% identical with that of *P. putida* mt-2 4-OT (58% similar).¹⁵ The TomN sequence has Pro-1, Arg-11, and Arg-39, which have been identified as critical residues for 4-OT and hh4-OT activity. Like that in hh4-OT, a tryptophan residue replaces Phe-50 of 4-OT in TomN.¹⁵

TomN is most similar to the α -subunits of the six previously identified hh4-OT homologues (38–50% identical sequence and 51–69% similar), followed by the 4-OT isozymes from *P. putida* mt-2 and *Pseudomonas* sp. CF600 (sequence 30% identical and 59% similar with that of *Pseudomonas* sp.

CF600).¹⁵ TomN is less similar with the β -subunits of these hh4-OT homologues (27–37% identical sequence and 41–48% similar). TomN also showed similarity with a 4-OT domain in a putative indigoidine synthase (IndC) from *Streptomyces clavuligerus* (27% identical sequence and 38% similar) and a related hypothetical protein (designated PAU_02638) from the human pathogen *Photobacterium asymbiotica* (33% identical sequence and 67% similar).^{33,34} Indigoidine is a blue pigment that may protect the host organism from oxidative stress and pathogenicity. Finally, the sequence of TomN is 29% identical and 47% similar with that of the α -subunit of *trans*-3-chloroacrylic acid dehalogenase (CaaD) and lacks detectable levels identity or similarity with the β -subunit of CaaD, another known heterohexamer in the tautomerase superfamily.³⁵

Kinetic Characterization of TomN. The proposed substrate for TomN (i.e., **2** in Scheme 1) is not available.¹ Hence, the TomN protein was examined for activity with known tautomerase superfamily substrates, including 2-hydroxy-muconate [**4** (Scheme 3)], 5-(methyl)-2-hydroxymuconate (**6**), 5-(carboxymethyl)-2-hydroxymuconate (**8**), 2-hydroxy-2,4-pentadienoate (**9**), 2-hydroxy-2,4-heptadiene-1,7-dioate (**12**), and phenylolnolpyruvate (**15**).^{36,37} TomN showed 1,5-keto–enol tautomerization activity with **4** and **6**, and 1,3-keto–enol tautomerization activities with **6** (data not shown), **9**, and **15** (Table 1). The enzyme does not process **8**. TomN processes **12** to **13**, but the kinetic data could not be fit to the Michaelis–Menten equation because consistent results could not be obtained at higher substrate concentrations.

The catalytic efficiency of TomN with **4** is slightly lower than those of canonical 4-OT and hh4-OT. The *K*_m value is elevated and *k*_{cat} value reduced, resulting in 18-fold (4-OT) and 12-fold (hh4-OT) lower *k*_{cat}/*K*_m values.¹⁵ Likewise, the catalytic efficiency of TomN with **6** is slightly less than that of 4-OT. The *K*_m value is elevated (2.5-fold) and the *k*_{cat} value reduced (12.6-fold), resulting in a 31-fold lower *k*_{cat}/*K*_m value. The catalytic efficiency of 4-OT using **9**, and converting it to **10**, is ~280-fold higher than that of TomN. The difference is primarily due to the 195-fold higher *k*_{cat} value measured for 4-OT. TomN does not process **9** to **11** or **12** to **14** at concentrations where the analogous 4-OT-catalyzed reactions have converted all substrate to product. The catalytic efficiency of TomN with **15** is comparable to that of hh4-OT but is ~8-fold lower than that of 4-OT. The difference is due primarily to the 5-fold higher *k*_{cat} value measured for 4-OT.

Kinetic Characterization of the TomN Mutants. Our previous work on 4-OT and hh4-OT indicated that Pro-1, Arg-11, and Arg-39 (β Pro-1, α Arg-12, and α Arg-40, respectively, in hh4-OT) played key roles in the enzyme-catalyzed reaction using **4**.^{7–12,15} Hence, these residues were replaced with alanine in TomN individually, and the kinetic parameters of the resulting mutant enzymes were determined using **4** as a substrate (Table 2). There are significant effects on the *k*_{cat} and *k*_{cat}/*K*_m values. Replacing Pro-1, Arg-11, and Arg-39 with alanines results in 1230-, 130-, and 9250-fold decreases in *k*_{cat}, respectively. Less significant changes are seen in the *K*_m values (a 2.3-fold decrease for the P1A mutant, a 2-fold increase for the R11A mutant, and a comparable value for the R39A mutant). As a result, the *k*_{cat}/*K*_m values for the three mutant enzymes are decreased 430-, 280-, and 8000-fold, respectively, and are a reflection (primarily) of the decreased *k*_{cat}. The most notable effects are the increase in the *K*_m value for the R11A

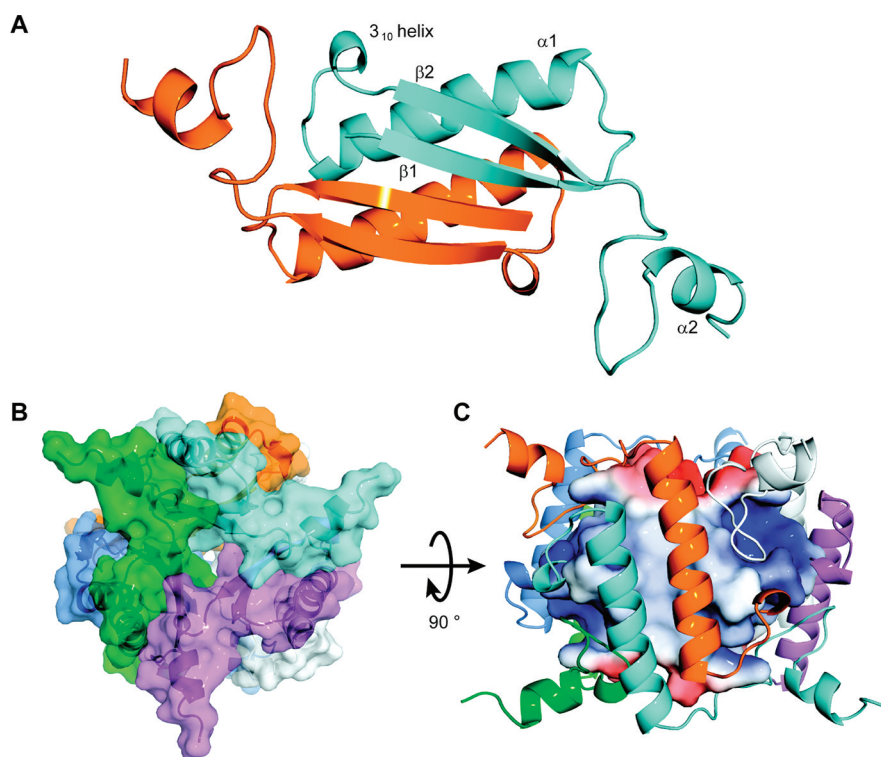


Figure 1. Structural overview of TomN. (A) Model of the TomN dimer showing the antiparallel β -sheets in front of the two α -helices. The two monomers are colored orange and cyan. The β - α - β signature fold for one monomer is shown as $\beta 1$, $\alpha 1$, and $\beta 2$. The short 3_{10} -helix that precedes strand $\beta 2$ and the C-terminal $\alpha 2$ helix are also shown. (B) Overall architecture of the TomN hexamer. A top view of the TomN hexamer where the six monomers making up the homohexamer are colored orange, cyan, blue, green, white, and magenta (counterclockwise). (C) Side view of the TomN hexamer (90° rotation from panel B) with the outer α -helices colored as in panel B. The inner β -strands are shown as the electrostatic surface potentials, where blue indicates positive charge, red indicates negative charge, and white indicates hydrophobic regions. The figures were generated with PyMoL.³² The surfaces were generated with the Adaptive Poisson–Boltzmann Solver (APBS)³⁹ using the AMBER force field (APBS Tools 2.1 PyMoL plugin, M. G. Lerner) and the conversion program known as PDB2PQR.^{40,41}

mutant and the marked decrease in the k_{cat} value for the R39A mutant.

The R61A mutant of TomN was also constructed and examined for activity using **4**. Our previous work on 4-OT did not implicate this residue in the mechanism,^{11,20} but the position of Arg-61 in the TomN crystal structure (*vide infra*) suggested a possible contribution. However, the changes in the kinetic parameters for the R61A mutant are not significant: there is a 5-fold decrease in k_{cat} and little change in K_{m} . The overall result is an 8-fold reduction in $k_{\text{cat}}/K_{\text{m}}$. This result suggests that Arg-61 plays a relatively marginal role in catalysis even though it is in the proximity of the active site. This analysis does not rule out a more direct role for Arg-61 with the biological substrate.

Inactivation of TomN by 2-Oxo-3-pentynoate (**17**).

Previous work showed that the reaction of **17** (Scheme 4) with tautomerase superfamily members reflects the ionization state of Pro-1.³⁶ The compound is a potent active site-directed irreversible inhibitor of 4-OT,²⁰ whereas CaaD, *cis*-3-chloroacrylic acid dehalogenase (*cis*-CaaD), and malonate semialdehyde decarboxylase (MSAD) catalyze the hydration of **17** to yield acetopyruvate (**18**) (Scheme 4).^{23,36,37} CaaD, *cis*-CaaD, and MSAD are found in a pathway for the catabolism of 1,3-dichloropropene.³⁷ The different reactivities of **17** correlate with the different $\text{p}K_{\text{a}}$ values of Pro-1. In 4-OT, Pro-1 has a $\text{p}K_{\text{a}}$ of ~ 6.4 so that it functions largely as a base and attacks **17** at C-4 in a Michael-type reaction.²⁰ In the three other enzymes, Pro-1 is largely cationic and cannot function as a

nucleophile.^{23,36,37} Instead, the compound is hydrated because the active site is designed to conduct a hydration reaction. We find that TomN is inactivated by **17**. Moreover, MALDI-MS analysis of the peptide mixture resulting after proteolysis (using protease V-8) indicates that Pro-1 is the site of covalent modification. The spectrum shows two signals: one signal that corresponds to the unmodified peptide Pro-1–Glu-9 (1053.52 Da) and the other signal that corresponds to the same peptide modified after incubation with **17** (1169.55 Da). The mass difference between the two peaks is 116.03 Da, which is consistent with the covalent modification of TomN by **17** at Pro-1.²⁰ These observations indicate that TomN, like 4-OT, functions as a tautomerase, and that Pro-1 likely has a $\text{p}K_{\text{a}}$ value comparable to that of Pro-1 in 4-OT.

Crystal Structure of TomN. The structure shows that TomN is constructed from the signature tautomerase superfamily β - α - β fold (Figure 1A).^{7,37,38} Two TomN monomers align in an inverted manner to form a dimer (Figure 1A). The quaternary structure can be viewed as a trimer of dimers where the inner core of the hexamer is formed by the parallel β -strands that dimerize at the interface (Figure 1B). The long α -helices ($\alpha 1$ from each dimer) constitute the outer wall of the hexamer and have short C-terminal α -helices ($\alpha 2$ from each monomer) that extend to the neighboring dimer and provide a lid to the active site for the neighboring molecule (Figure 1C). The β -sheets from two monomers form a four-stranded antiparallel β -sheet on one side, while two antiparallel α -helices are on the other side. The hydrogen bonds formed by the two

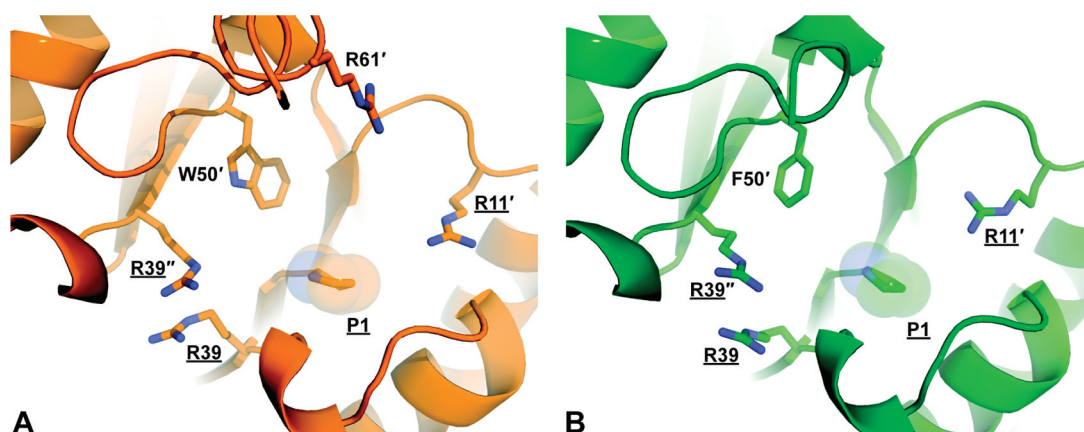


Figure 2. Comparison of the TomN (orange) and 4-OT (green) active sites. (A) Active site of TomN showing the catalytically required residues (underlined) from three different monomers (designated by primes) as sticks. (B) Active site of 4-OT showing the catalytically required residues (underlined) from three different monomers (designated by primes) as sticks.

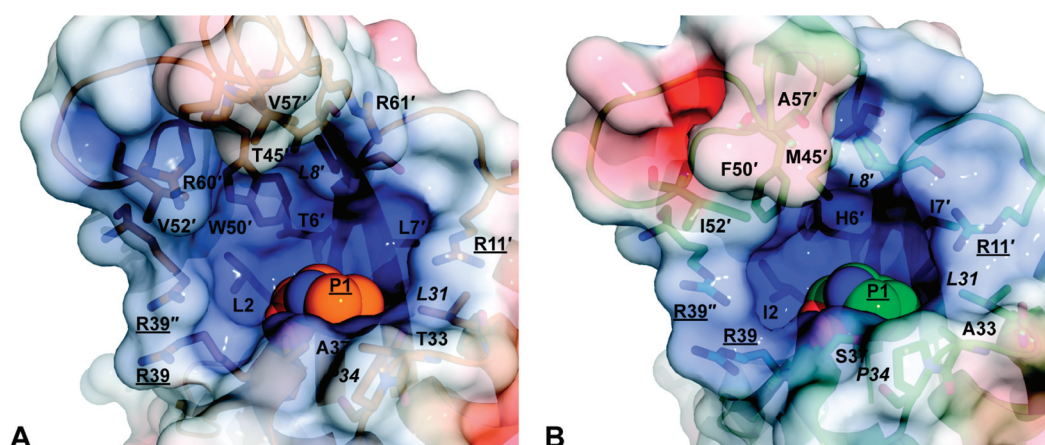


Figure 3. Detailed comparison of the TomN and 4-OT active sites with the electrostatic surface potentials shown. (A) Electrostatic surface potential of the TomN active site. Residues that define the active site pocket are represented as sticks and are labeled as in Figure 2. The italicized labels indicate identical residues between the two proteins. (B) Electrostatic surface potential of the 4-OT active site. In both panels, blue indicates positive charge, red indicates negative charge, and white indicates hydrophobic regions. Surfaces were generated as described in the legend of Figure 1.

antiparallel β -sheets stabilize the dimer. The core structure is comparable to that of 4-OT and hh4-OT.^{15,20}

The active site in both TomN (Figure 2A) and 4-OT (Figure 2B) (PDB code: 1BJP) is a cavity on the surface created by the ends of the β -strands of two neighboring dimers. In TomN, the active site contains Pro-1 and Arg-39 from one monomer, Arg-11', Arg-61', and Trp-50' from the neighboring monomer of the dimer, and Arg-39'' (primed residues refer to different subunits in TomN) from the neighboring dimer (Figure 2A). This active site configuration mirrors that of 4-OT (with the exception of Trp-50' and Arg-61'). Each active site is polarized with the positively charged arginine residues at either end (i.e., Arg-11' at one end and Arg-39 at the other end) and the catalytic Pro-1 roughly spaced between them. Importantly, the highly similar structure and orientation of the active sites are entirely consistent with the preceding sequence, kinetic, and mutagenic analysis.

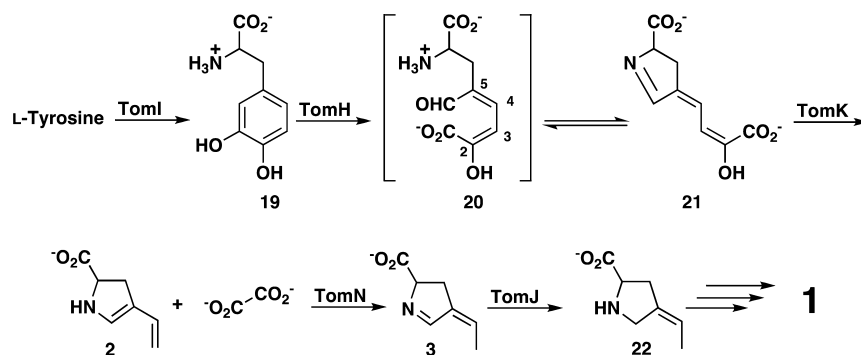
A detailed examination of the active sites shows that the residues are mostly identical or very similar (Figure 3A,B). The larger bulk of Trp-50 (Phe-50 in 4-OT) is accommodated by the replacement of Met-45 (4-OT) with Thr-45. However, one difference (Val-52 in place of Ile-52) may render the TomN active site slightly more accommodating than that of 4-OT

(Figure 3A,B). Overall, these changes suggest subtle differences in the active sites. The electrostatic potential surface shows that the charge distribution (positive, negative, and hydrophobic) is comparable in the two active sites.

DISCUSSION

Three 4-OTs (defined by their ability to convert 4 to 5) have now been characterized: the homohexamer 4-OT from *P. putida* mt-2, the heterohexamer 4-OT from *C. aurantiacus* J-10-fl, and the homohexamer TomN from *Streptomyces achromogenes*.^{4,6,7,15} (The 4-OT isozyme from *Pseudomonas* sp. CF600 is not considered in this discussion because it is so similar to *P. putida* mt-2 4-OT.⁷) Although they all catalyze the canonical 4-OT reaction with similar efficiencies, there are two distinctions. First, TomN probably has a different biological substrate. Second, the homo- and heterohexamer 4-OTs are found in catabolic pathways and TomN is found in a biosynthetic pathway that, at first glance, has a few parallel reactions to those found in the catabolic pathways.^{1,6,15}

The *P. putida* mt-2 4-OT is part of a so-called catechol meta-fission pathway, which is a bacterial catabolic pathway that transforms simple aromatic hydrocarbons such as benzene, toluene, and xylenes into useful cellular intermediates.^{6,7} The

Scheme 5. Proposed Sequence of Events Converting L-Tyrosine to the C Ring of Tomaymycin¹


presence of this pathway allows the host bacteria to use these compounds as their sole sources of carbon and energy. The enzyme is a homohexamer with six active sites, which consist of residues from three adjoining monomers.^{6,20}

A structural variation of the homohexamer 4-OT was discovered in the thermophilic bacteria *C. aurantiacus* J-10-fl.¹⁵ The hh4-OT consists of α - and β -subunits (forming a functional $\alpha\beta$ -dimer), in which the α -subunit, which does not have an amino-terminal proline, is annotated as a tautomerase-like protein.¹⁵ The β -subunit provides the catalytic amino-terminal proline. The hh4-OT is part of a meta-fission pathway based on its genomic context, but this has not been confirmed by biochemical characterization of the enzymes. Other than the quaternary structure, the factors conferring thermostability, and the absence of the low-level dehalogenase activity, the mechanistic and kinetic properties of hh4-OT largely resemble those of 4-OT.¹⁵ In both 4-OT and hh4-OT, Pro-1 (β Pro-1), Arg-11 (α Arg-12), and Arg-39 (α Arg-40) have been identified as key catalytic residues.

TomN is found in a biosynthetic pathway, but some of the initial reaction chemistry for the proposed ring C biosynthesis seemingly parallels that typically found in meta-fission degradative pathways (Scheme 5).¹ For example, the second step in the proposed five-step biosynthetic sequence involves oxidative extradiol aromatic ring cleavage of L-Dopa.⁴² The third step is an enzyme-catalyzed hydrolytic cleavage of the dienol ring-fission product.⁴³ TomN is then proposed to tautomerize the product (i.e., 2). However, these assigned functions are tentative, and with the exception of TomN, the biochemical characterization of the enzymes is only in the very early stages. Moreover, the dioxygenase (TomH) and hydrolase (TomK) show no detectable sequence identity with the enzymes in various meta-fission pathways. Like 4-OT, TomN is a homohexamer, and Pro-1 and two arginine residues are critical for activity.

The mutagenesis experiments indicate that Pro-1, Arg-11, and Arg-39 in TomN play roles analogous to those proposed for these residues in *P. putida* mt-2 4-OT and hh4-OT (in the conversion of 4 to 5) (Table 2). Accordingly, replacing Pro-1 with an alanine affects k_{cat} more significantly than K_{m} , and this substantial decrease is the primary factor responsible for the decrease in $k_{\text{cat}}/K_{\text{m}}$. The decrease in k_{cat} can be ascribed to an effect on the reaction chemistry, product release, or both. Alanine is less basic and more flexible than proline, so that the decrease in basicity along with the suboptimal positioning of the base could account for the reduced activity of the mutant.¹⁰ The decrease in K_{m} could be due to the removal of the "bulky" ring of proline, making more room for the substrate. Similar

results were obtained for the P1A mutant of 4-OT and hh4-OT, except the decrease in k_{cat} for TomN is ~ 10 -fold greater.^{10,15} The results are consistent with the role of Pro-1 as a base in the reaction. Changing Arg-11 to an alanine impacts both K_{m} and k_{cat} , and this follows the same trend observed for 4-OT and hh4-OT. As would be anticipated for the removal of the group involved in C-6 carboxylate binding, the K_{m} increases. Likewise, the k_{cat} decreases because alanine cannot draw electron density away from C-5 and facilitate protonation. Finally, changing Arg-39 to an alanine has a profound effect on k_{cat} and an only minimal effect on K_{m} . The decrease in k_{cat} is much more dramatic than that observed for the other 4-OTs, suggesting that Arg-39 plays a much more substantial role in catalysis.^{11,15}

In 4-OT, Pro-1 can function as a base because it has a $\text{p}K_{\text{a}}$ value of ~ 6.4 , which is due in part to the presence of Phe-50.¹³ The side chain of Phe-50 creates a nearby pocket of hydrophobicity. The inactivation of TomN by 2-oxo-3-pentynoate (17) by the covalent modification of the prolyl nitrogen suggests that the $\text{p}K_{\text{a}}$ of Pro-1 is comparable to that of 4-OT (also inactivated by 17). The crystal structure places Trp-50 in a position identical to that of Phe-50 in 4-OT, suggesting a similar role (Figures 2 and 3).

Two observations from the substrate specificity studies may provide clues about the properties of a biological substrate for TomN. First, 4 is an excellent substrate for TomN. However, with the exception of 4 and 6, TomN is not particularly efficient in conducting 1,5-keto-enol tautomerization reactions (to produce the so-called conjugated ketones) with two other dienols (9 and 12) used in this study, whereas 4-OT is.^{11,16,19} This observation is somewhat surprising, but it could suggest that subtle differences in TomN preclude the efficient formation of conjugated ketones from dienols and that the biological function for TomN does not involve this type of reaction. Second, TomN, like 4-OT, processes mono- and diacid compounds, although for both enzymes the monoacids (9 and 15) are not processed as efficiently as the diacids (4 and 6).¹⁵ A future stereochemical analysis will show if the substrates bind similarly in the two active sites.^{5,11,16,17}

The crystal structure of TomN shows that it largely resembles those of 4-OT and the hh4-OT, with main chain rmsd's of 0.8 and 1.1 Å, respectively.^{7,15,20} The active sites are nearly identical, and the key residues are positionally conserved (Figure 2). The structure of TomN and the conservation of essential catalytic residues suggest that similar catalytic and substrate recognition mechanisms are used in the three enzymes and are fully consistent with the kinetic and mutagenic results.

On the basis of the kinetic, mechanistic, and structural results presented here, it is apparent that TomN functions very much like a canonical 4-OT, processing **4** to **5**. Subtle differences in the active site of TomN could account for the different kinetic parameters obtained for the various substrates. These results have two implications. First, the striking similarities question whether the proposed substrate for TomN (i.e., **2**) is, in fact, the biological substrate or whether TomN processes a substrate that more closely resembles **4**. Second, if **2** is not the substrate for TomN, then the proposed role for the TomN reaction in the biosynthetic pathway for the C ring of **1** may not be correct, and the proposed steps leading to ring formation may have to be re-examined.

In the currently proposed version, tyrosine is hydroxylated to yield L-Dopa [**19** (Scheme 5)] (ref 1 and unpublished data of K. L. Conner and B. Gerratana, 2011). L-Dopa undergoes meta fission (catalyzed by TomH) to produce (presumably) initially **20**, which is proposed to cyclize to the dihydropyrrolidine species **21**.¹ The subsequent TomK-catalyzed reaction yields oxalate and **2**, the putative substrate for TomN. Tautomerization by TomN affords **3**, which is reduced by the F420-dependent enzyme, TomJ, to generate **22**. A series of reactions then incorporates **22** into the tricyclic ring system to yield **1**.¹ It should be emphasized that these assignments are tentative and are not based on extensive biochemical characterization of the individual enzymes.

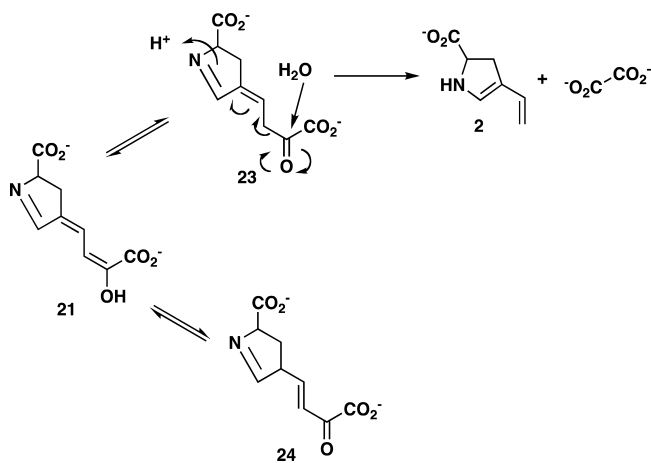
The proposed conversion of **19** to **22** poses three potential problems (Scheme 5). First, the electron donating properties of

the 2-hydroxy group (in **20**) could attenuate the electrophilicity of the aldehyde carbonyl group and preclude a spontaneous ring closure (to **21**) or make spontaneous ring closure a slow process.⁴⁴ Second, dienols (such as **20** or **21**) are likely in equilibrium with their 1,3- and 1,5-keto-enol tautomers [**23** and **24** (Scheme 6)].⁴⁵ Hydrolytic cleavage (by TomK) most reasonably occurs via the 1,3 tautomer (i.e., **23**), yet the reaction with **4** suggests that **24** might be favored. Third, compounds **21** and **3** could be in equilibrium with the acyclic counterparts such that the assignment of a substrate to an enzyme is compounded further. The reduction of **3** by TomJ might ultimately drive the pathway forward to converge on **22**.

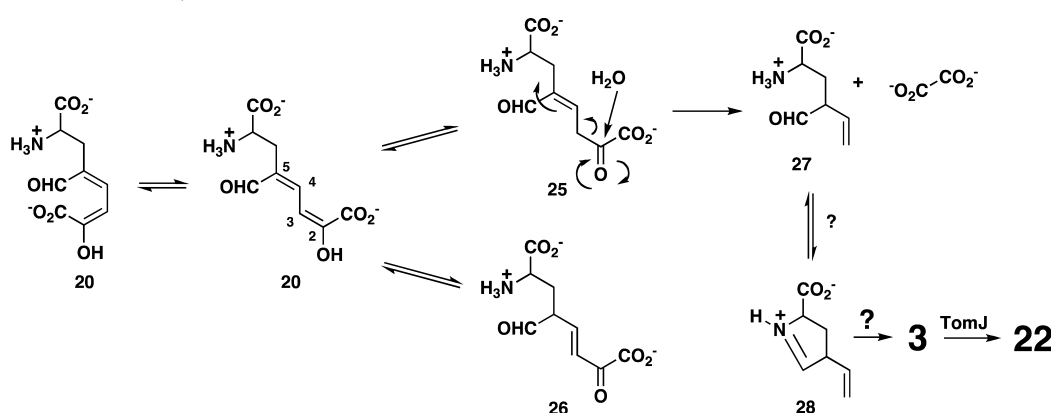
One possible alternative reaction sequence, which addresses some issues, is shown in Scheme 7. Ring opening again yields **20**, which presumably exists in the *s-trans* form. TomN could then tautomerize **20** (which has the 2-hydroxymuconate framework) to **25** or **26**. Although protonation can occur at C-3 (to yield **25**) or C-5 (to yield **26**), steric hindrance at C-5 (the aldehyde and amino acid moieties) might preclude C-5 protonation and favor formation of **25**.⁴⁵ Moreover, TomN could favor one tautomer (i.e., **25**) so that a wasteful nonenzymatic partitioning of the reactive **20** to both isomers is minimized. If the reaction proceeds via **25**, TomK can then carry out a hydrolytic cleavage and produce **27** and oxalate, a known product of the pathway. A spontaneous ring closure of **27** to **28** is more likely (than that of **20** to **21**), with **27** and **28** in equilibrium. If **3** is the substrate for TomJ (and **22** is the product), then a 1,3-allylic rearrangement of **28** to **3** is required at this stage. It is not known if and how this happens. In one variation of this pathway, TomK could be responsible for the ketonization of **20** to **25**, the hydrolytic cleavage of **25** to **27**, and ring closure.⁴³ In this scenario, TomN is available to convert **28** to **3**. Clearly, the chemistry of the pathway intermediates is complex and must be sorted out before definitive roles can be assigned to the enzymes.

It remains a possibility that TomN processes **2** to **3**. The substrate specificity studies do not rule out the processing of monoacids. The appropriate experiment will be conducted when and if **2** can be generated (most likely, in situ from **19**). In the absence of the genomic and pathway context, TomN might have been misannotated as a 4-OT on the basis of its sequence similarity to the 4-OT family and its activity with **4**. This raises the question of whether several enzymes annotated as “4-OTs” that lack an operon context actually conduct different biological reactions. This observation underscores the difficulty of functional annotation because the subtle sequence

Scheme 6. Tautomers of 21 and Carbon–Carbon Bond Fission of 23



Scheme 7. Alternative Pathway for the Conversion of 20 to 22



and structural features defining the individual reaction and substrate specificities are not yet known.

One reason for characterization of the tomaymycin biosynthetic cluster is to produce more potent tomaymycin analogues that lack the dose-limiting toxicity.¹ If this is to become a reality, the actual sequence of events must be established for the pathway (including the steps resulting in C ring construction). In addition, a more detailed understanding of the chemistry must be obtained, including an improved understanding of how substituents affect the reactivity of **20** and **21** (if **21** is generated) and the equilibrium of acyclic and cyclic forms of proposed intermediates along the pathway (e.g., **20** and **21** or **27** and **28**). Efforts are now underway to do this.

■ ASSOCIATED CONTENT

Accession Codes

The atomic coordinates and structure factors have been deposited with the Brookhaven Protein Data Bank (entry 3ry0).

■ AUTHOR INFORMATION

Corresponding Author

*Y.Z.: telephone, (512) 471-8645; e-mail, jzhang@cm.utexas.edu. C.P.W.: telephone, (512) 471-6198; fax, (512) 232-2606; e-mail, whitman@mail.utexas.edu.

Funding

This research was supported by National Institutes of Health Grants GM-41239 (C.P.W.) and GM-084473 (B.G.), a fellowship award (F32 GM089083) from the National Institute of General Medical Sciences (G.K.S.), and Robert A. Welch Foundation Grant F-1334 (C.P.W.).

■ ACKNOWLEDGMENTS

We thank Steve D. Sorey (Department of Chemistry, University of Texas) for his expert assistance in the acquisition of the ¹H NMR spectra.

■ ABBREVIATIONS

CaaD and *cis*-CaaD, *trans*- and *cis*-3-chloroacrylic acid dehalogenase, respectively; ESI, electrospray ion-trap; HEPES, *N*-(2-hydroxyethyl)piperazine-*N'*-2-ethanesulfonate; IPTG, isopropyl β -D-thiogalactoside; Kn, kanamycin; LB, Luria-Bertani; MALDI, matrix-assisted laser desorption ionization; MSAD, malonate semialdehyde decarboxylase; MR, molecular replacement; NMR, nuclear magnetic resonance; 4-OT, 4-oxalocrotonate tautomerase; PEG, polyethylene glycol; PCR, polymerase chain reaction; PBD, pyrrolo[1,4]benzodiazepine; rms, root-mean-square; SDS-PAGE, sodium dodecyl sulfate-polyacrylamide gel electrophoresis.

■ REFERENCES

- (1) Li, W., Chou, S. C., Khullar, A., and Gerratana, B. (2009) Cloning and characterization of the biosynthetic cluster for tomaymycin, an SJG-136 monomeric analog. *Appl. Environ. Microbiol.* 75, 2958–2963.
- (2) Li, W., Khullar, A., Chou, S. C., Sacramo, A., and Gerratana, B. (2009) Biosynthesis of sibiromycin, a potent antitumor antibiotic. *Appl. Environ. Microbiol.* 75, 2869–2878.
- (3) Gerratana, B. (2010) Biosynthesis, synthesis, and biological activities of pyrrolobenzodiazepines. *Med. Res. Rev.*, DOI: DOI: 10.1002/med.20212.

- (4) Whitman, C. P., Aird, B. A., Gillespie, W. R., and Stolowich, N. J. (1991) Chemical and enzymatic ketonization of 2-hydroxymuconate, a conjugated enol. *J. Am. Chem. Soc.* 113, 3154–3162.
- (5) Wang, S. C., Johnson, W. H. Jr., Czerwinski, R. M., Stamps, S. L., and Whitman, C. P. (2007) Kinetic and stereochemical analysis of YwhB, a 4-oxalocrotonate tautomerase homologue in *Bacillus subtilis*: Mechanistic implications for the YwhB- and 4-oxalocrotonate tautomerase-catalyzed reactions. *Biochemistry* 46, 11919–11929.
- (6) Harayama, S., Rekik, M., Ngai, K.-L., and Ornston, L. N. (1989) Physically associated enzymes produce and metabolize 2-hydroxy-2,4-dienoate, a chemically unstable intermediate formed in catechol metabolism via *meta* cleavage in *Pseudomonas putida*. *J. Bacteriol.* 171, 6251–6258.
- (7) Subramanya, H. S., Roper, D. I., Dauter, Z., Dodson, E. J., Davies, G. J., Wilson, K. S., and Wigley, D. B. (1996) Enzymatic ketonization of 2-hydroxymuconate: Specificity and mechanism investigated by the crystal structures of two isomerases. *Biochemistry* 35, 792–802.
- (8) Stivers, J. T., Abeygunawardana, C., Mildvan, A. S., Hajipour, G., Whitman, C. P., and Chen, L. H. (1996) Catalytic role of the amino-terminal proline in 4-oxalocrotonate tautomerase: Affinity labeling and heteronuclear NMR studies. *Biochemistry* 35, 803–813.
- (9) Stivers, J. T., Abeygunawardana, C., Mildvan, A. S., Hajipour, G., and Whitman, C. P. (1996) 4-Oxalocrotonate tautomerase: pH dependences of catalysis and pK_a values of active site residues. *Biochemistry* 35, 814–823.
- (10) Czerwinski, R. M., Johnson, W. H. Jr., Whitman, C. P., Harris, T. K., Abeygunawardana, C., and Mildvan, A. S. (1997) Kinetic and structural effects of mutations of the catalytic amino-terminal proline in 4-oxalocrotonate tautomerase. *Biochemistry* 36, 14551–14560.
- (11) Harris, T. K., Czerwinski, R. M., Johnson, W. H. Jr., Legler, P. M., Abeygunawardana, C., Massiah, M. A., Stivers, J. T., Whitman, C. P., and Mildvan, A. S. (1999) Kinetic, stereochemical, and structural effects of mutations of the active site arginine residues in 4-oxalocrotonate tautomerase. *Biochemistry* 38, 12343–12357.
- (12) Czerwinski, R. M., Harris, T. K., Johnson, W. H. Jr., Legler, P. M., Stivers, J. T., Mildvan, A. S., and Whitman, C. P. (1999) Effects of mutations of the active site arginine residues in 4-oxalocrotonate tautomerase on the pK_a values of active site residues and on the pH dependence of catalysis. *Biochemistry* 38, 12358–12366.
- (13) Czerwinski, R. M., Harris, T. K., Massiah, M. A., Mildvan, A. S., and Whitman, C. P. (2001) The structural basis for the perturbed pK_a of the catalytic base in 4-oxalocrotonate tautomerase: Kinetic and structural effects of mutations of Phe-50. *Biochemistry* 40, 1984–1995.
- (14) Wang, S. C., Johnson, W. H. Jr., and Whitman, C. P. (2003) The 4-oxalocrotonate tautomerase- and YwhB-catalyzed hydration of 3E-haloacrylates: Implications for evolution of new enzymatic activities. *J. Am. Chem. Soc.* 125, 14282–14283.
- (15) Burks, E. A., Fleming, C. D., Mesecar, A. D., Whitman, C. P., and Pegan, S. D. (2010) Kinetic and structural characterization of a heterohexameric 4-oxalocrotonate tautomerase from *Chloroflexus aurantiacus* J-10-fl: Implications for functional and structural diversity in the tautomerase superfamily. *Biochemistry* 49, 5016–5027.
- (16) Lian, H., Czerwinski, R. M., Stanley, T. M., Johnson, W. H. Jr., Watson, R. J., and Whitman, C. P. (1998) The contribution of the substrate's carboxylate group to the mechanism of 4-oxalocrotonate tautomerase. *Bioorg. Chem.* 26, 141–156.
- (17) Hajipour, G., Johnson, W. H. Jr., Dauben, P. D., Stolowich, N. J., and Whitman, C. P. (1993) Chemical and enzymatic ketonization of 5-(carboxymethyl)-2-hydroxymuconate. *J. Am. Chem. Soc.* 115, 3533–3542.
- (18) Stanley, T. M., Johnson, W. H. Jr., Burks, E. A., Whitman, C. P., Hwang, C.-C., and Cook, P. F. (2000) Expression and stereochemical and isotope effect studies of active 4-oxalocrotonate decarboxylase. *Biochemistry* 39, 718–726.

- (19) Burks, E. A., Johnson, W. H. Jr., and Whitman, C. P. (1998) Stereochemical and isotopic labeling studies of 2-oxo-hept-4-ene-1,7-dioate hydratase: Evidence for an enzyme-catalyzed ketonization step in the hydration reaction. *J. Am. Chem. Soc.* 120, 7665–7675.
- (20) Taylor, A. B., Czerwinski, R. M., Johnson, W. H. Jr., Whitman, C. P., and Hackert, M. L. (1998) Crystal structure of 4-oxalocrotonate tautomerase inactivated by 2-oxo-3-pentynoate at 2.4 Å resolution: Analysis and implications for the mechanism of inactivation and catalysis. *Biochemistry* 37, 14692–14700.
- (21) Poelarends, G. J., Almrud, J. J., Serrano, H., Darty, J. E., Johnson, W. H. Jr., Hackert, M. L., and Whitman, C. P. (2006) Evolution of enzymatic activity in the tautomerase superfamily: Mechanistic and structural consequences of the L8R mutation in 4-oxalocrotonate tautomerase. *Biochemistry* 45, 7700–7708.
- (22) Sambrook, J., Fritsch, E. F., and Maniatis, T. (1989) *Molecular Cloning: A Laboratory Manual*, 2nd ed., Cold Spring Harbor Laboratory Press, Plainview, NY.
- (23) Wang, S. C., Person, M. D., Johnson, W. H. Jr., and Whitman, C. P. (2003) Reactions of *trans*-3-chloroacrylic acid dehalogenase with acetylene substrates: Consequences of and evidence for a hydration reaction. *Biochemistry* 42, 8762–8773.
- (24) Waddell, W. J. (1956) A simple ultraviolet spectrophotometric method for the determination of protein. *J. Lab. Clin. Med.* 48, 311–314.
- (25) Schagger, H., and von Jagow, G. (1987) Tricine-sodium dodecyl sulfate-polyacrylamide gel electrophoresis for the separation of proteins in the range of 1 to 100 kDa. *Anal. Biochem.* 166, 368–379.
- (26) Ho, S. N., Hunt, H. D., Horton, R. M., Pullen, J. K., and Pease, L. R. (1989) Site-directed mutagenesis by overlap extension using the polymerase chain reaction. *Gene* 77, 51–59.
- (27) Taylor, A.B., Johnson, W. H. Jr., Czerwinski, R. M., Li, H.-S., Hackert, M. L., and Whitman, C. P. (1999) Crystal structure of macrophage migration inhibitory factor complexed with (*E*)-2-fluoro-*p*-hydroxycinnamate at 1.8 Å resolution: Implications for enzymatic catalysis and inhibition. *Biochemistry* 38, 7444–7452.
- (28) Bradford, M. M. (1976) A rapid and sensitive method for the quantitation of microgram quantities of protein utilizing the principle of protein-dye binding. *Anal. Biochem.* 72, 248–254.
- (29) Otwinowski, Z., and Minor, W. (1997) Processing of X-ray diffraction data collected in oscillation mode. *Methods Enzymol.* 276, 307–326.
- (30) Collaborative Computational Project, Number 4 (1994) The CCP4 suite: Programs for protein crystallography. *Acta Crystallogr. D* 50, 760–763.
- (31) Laskowski, R. A., MacArthur, M. W., Moss, D. S., and Thornton, J. M. (1993) PROCHECK: A program to check the stereochemical quality of protein structures. *J. Appl. Crystallogr.* 26, 283–291.
- (32) DeLano, W. L. (2002) *The PyMol Molecular Graphics System*, DeLano Scientific, San Carlos, CA.
- (33) Medema, M. H., Trefzer, A., Kovalchuk, A., van den Berg, M., Müller, U., Heijne, W., Wu, L., Alam, M. T., Ronning, C. M., Nierman, W. C., Bovenberg, R. A., Breitling, R., and Takano, E. (2010) The sequence of a 1.8-mb bacterial linear plasmid reveals a rich evolutionary reservoir of secondary metabolic pathways. *Genome Biol. Evol.* 2, 212–224.
- (34) Wilkinson, P., Waterfield, N. R., Crossman, L., Corton, C., Sanchez-Contreras, M., Vlisidou, I., Barron, A., Bignell, A., Clark, L., Ormond, D., Mayho, M., Bason, N., Smith, F., Simmonds, M., Churcher, C., Harris, D., Thompson, N. R., Quail, M., Parkhill, J., and Ffrench-Constant, R. H. (2009) Comparative genomics of the emerging human pathogen *Photobacterium luminescens* with the insect pathogen *Photobacterium luminescens*. *BMC Genomics* 10, 302.
- (35) Poelarends, G. J., Saunier, R., and Janssen, D. B. (2001) *trans*-3-Chloroacrylic acid dehalogenase from *Pseudomonas pavonaceae* 170 shares structural and mechanistic similarities with 4-oxalocrotonate tautomerase. *J. Bacteriol.* 183, 4269–4277.
- (36) Poelarends, G. J., Serrano, H., Johnson, W. H. Jr., Hoffman, D. W., and Whitman, C. P. (2004) The hydratase activity of malonate semialdehyde decarboxylase: Mechanistic and evolutionary implications. *J. Am. Chem. Soc.* 126, 15658–15659.
- (37) Poelarends, G. J., Veetil, V. P., and Whitman, C. P. (2008) The chemical versatility of the β - α - β fold: Catalytic promiscuity and divergent evolution in the tautomerase superfamily. *Cell. Mol. Life Sci.* 65, 3606–3618.
- (38) Whitman, C. P. (2002) The 4-oxalocrotonate tautomerase family of enzymes: How nature makes new enzymes using a β - α - β structural motif. *Arch. Biochem. Biophys.* 402, 1–13.
- (39) Baker, N. A., Sept, D., Joseph, S., Holst, M. J., and McCammon, J. A. (2001) Electrostatics of nanosystems: Application to microtubules and the ribosome. *Proc. Natl. Acad. Sci. U.S.A.* 98, 10037–10041.
- (40) Dolinsky, T. J., Czodrowski, P., Li, H., Nielsen, J. E., Jensen, J. H., Klebe, G., and Baker, N. A. (2007) PDB2PQR: Expanding and upgrading automated preparation of biomolecular structures for molecular simulations. *Nucleic Acids Res.* 35, W522–W525.
- (41) Dolinsky, T. J., Nielsen, J. E., McCammon, J. A., and Baker, N. A. (2004) PDB2PQR: An automated pipeline for the setup, execution, and analysis of Poisson-Boltzmann electrostatics calculations. *Nucleic Acids Res.* 32, W665–W667.
- (42) Bugg, T. D., and Ramaswamy, S. (2008) Non-heme iron-dependent dioxygenases: Unravelling catalytic mechanisms for complex enzymatic oxidations. *Curr. Opin. Chem. Biol.* 12, 134–140.
- (43) Li, C., Montgomery, M. G., Mohammed, F., Li, J. J., Wood, S. P., and Bugg, T. D. (2005) Catalytic mechanism of C-C hydrolase MhpC from *Escherichia coli*: Kinetic analysis of His263 and Ser110 site-directed mutants. *J. Mol. Biol.* 346, 241–251.
- (44) Colabroy, K. L., and Begley, T. P. (2005) The pyridine ring of NAD is formed by a nonenzymatic pericyclic reaction. *J. Am. Chem. Soc.* 127, 840–841.
- (45) Whitman, C. P. (1999) Keto-enol tautomerization in enzymatic reactions. In *Comprehensive Natural Products Chemistry* (Barton, D., and Nakanishi, K., Eds.) Vol. 5 (Poulter, C. D., Ed.), pp 31–50, Elsevier Science Ltd., Oxford, U.K.